

# Continuous Coating of Discrete Areas of a Flexible Web

C. L. Bower, E. A. Simister, E. Bonnist, K. Paul, N. Pightling, and T. D. Blake  
Kodak European Research, Cambridge CB4 0WN, U.K.

DOI 10.1002/aic.11215

Published online June 1, 2007 in Wiley InterScience (www.interscience.wiley.com).

*The use of surface energy (wettability) contrast to direct liquid into designated areas, so that flexible substrates can be coated with a discrete pattern in a continuous, roll-to-roll manner is described. The method makes use of a substrate prepatterned with lyophilic and lyophobic regions. When this substrate is over-coated with the target liquid, the liquid withdraws from the lyophobic areas and collects on the lyophilic ones. The surface-energy pattern and the liquid can be applied by a variety of different methods, but we have focused on printing the patterns by flexography and slide coating the target liquid. A benefit of the technique is that coatings of subsequent layers with the same pattern are self-aligned with the previous layer, since they are directed by the same surface energy pattern. The capability to perform simultaneous multi-layer patterned coating in a single-pass operation is also demonstrated. © 2007 American Institute of Chemical Engineers AICHE J, 53: 1644–1657, 2007*

**Keywords:** surface-energy contrast, patterned coating, contact angle, wetting, dewetting

## Introduction

Patterning based on surface energy contrast is already used in a variety of areas ranging from conventional process such as offset lithographic printing to modern applications in microfluidics<sup>1</sup> and hybrid inkjet patterning.<sup>2,3</sup> In lithographic printing, for example, the image areas are typically lyophobic and ink-receptive, whereas the nonimage areas are lyophilic and therefore receptive to the aqueous “fountain solution” used to maintain the lithographic differential. Here we describe a new application of these principles: continuous discrete coating (CDC). CDC is a method of coating discrete areas of a flexible substrate in a continuous, roll-to-roll manner, which uses differences in surface energy or wettability to direct the target liquid onto designated areas and so create precise well-defined patterns.<sup>4</sup>

The ability to coat discrete areas has obvious benefits. These include material savings and the possibility of fabricat-

ing complex layered structures. Existing discrete or “patch” coating methods typically rely on repeatedly starting and stopping the coating flow, or make use of printing techniques such as screen-printing or inkjet. CDC offers a new approach, which, in combination with existing methods, could facilitate low-cost manufacture of complex coated structures, such as displays.

The term “wetting” is commonly used to describe the displacement of air from a liquid or solid surface by water or another liquid. “Dewetting” is the reverse process. The contact angle ( $\theta$ ) is defined as the angle, measured through the liquid, between the solid surface and the tangent to the liquid surface at the three-phase contact line. As given by Young’s Eq. 1, the contact angle for a liquid drop resting on a plane solid surface is the result of the mechanical equilibrium of the three interfacial tensions acting at the contact line:

$$\gamma_{SV} - \gamma_{SL} = \gamma_{LV} \cos \theta \quad (1)$$

where  $\gamma_{SV}$ ,  $\gamma_{SL}$ , and  $\gamma_{LV}$  are the tensions of the solid–vapor, solid–liquid, and liquid–vapor interfaces, respectively. The smaller the contact angle, the better the liquid is said to wet the solid. A liquid with a zero contact angle is said to com-

This article contains supplementary material available via the Internet at <http://www.interscience.wiley.com/jpages/0001-1541/suppmat>.

Correspondence concerning this article should be addressed to C. L. Bower at [chris.bower@kodak.com](mailto:chris.bower@kodak.com).

pletely wet the solid. Interfacial tension is thermodynamically related to the specific surface free energy of the interface.<sup>5,6</sup> In simple cases, the two quantities are numerically equal, and so the terms are often used interchangeably.

To use surface energy patterning as a technique for coating discrete areas of a support, the wettability contrast should be maximized; in other words the contact angle of the coating solution on the lyophobic (i.e. hydrophobic or oleophobic) mask should be as large as possible, while that on the areas to be coated should be as small as possible, preferably 0. The selection of materials for the substrate and the lyophobic mask is therefore of paramount importance.

In the 1960s Zisman and Shafrin<sup>7</sup> used plots of the cosine of the contact angle against liquid surface tension to determine the critical surface tension of the solid surface  $\gamma_c$ , i.e. the surface tension of the liquid that would just completely wet the solid surface with a contact angle of zero degrees. Data for a homologous series of liquids such as the alkanes fall on a more-or-less straight line, the intercept of which on the  $\cos \theta = 0$  axis gives  $\gamma_c$ . This representation is known as a Zisman plot. A low value of  $\gamma_c$  indicates a poorly wetted surface with a low surface energy.

The critical surface tension also provides a practical means of correlating wettability with surface chemistry. Table 1 lists examples of some critical surface tensions and shows the effect of varying the chemical composition of the solid surface.

It can be seen that as the degree of fluorination increases,  $\gamma_c$  progressively decreases, indicating an increasingly less wettable surface. Fluorinated materials are therefore very useful in forming the lyophobic mask in CDC. However, the wettability of a solid by a liquid is determined not only by the various interfacial tensions according to Young's equation, but also by other factors such as surface roughness, chemical heterogeneity, and the presence of adsorbed layers. Such factors usually give rise to contact angle hysteresis, whereby the static contact angle can take any value between so-called advancing and receding limits,  $\theta_A$  and  $\theta_R$ , respectively. On polymer surfaces, in particular, changes in molecular orientation, swelling, partial dissolution, or the presence of low-molecular-weight constituents may also have to be taken into account.<sup>9</sup> These factors may therefore have to be considered when selecting materials for CDC.

### CDC concept

CDC involves the following steps, which are described with reference to Figure 1:

- Creating, on a continuous lyophilic web of support, a lyophobic mask, shown in grey, that defines the areas that ultimately will not be coated. The mask is then dried or cured (a).
- Coating the target solution, shown in black, onto the masked support (b).
- Destabilizing the solution layer so that it spontaneously rearranges, withdrawing from the lyophobic regions, to leave the coating on only the lyophilic cells.
- Allowing sufficient time for the target solution to recede from the masked areas and accumulate uniformly in the unmasked cells, and finally drying and/or curing the coated solution. (c).

**Table 1. Critical Surface Tension Values of Selected Surface Groups and Some Common Polymers Showing the Effect of Varying Degrees of Fluorination<sup>8</sup>**

| Surface Composition                | (mNrc m <sup>-1</sup> , 20°C) |
|------------------------------------|-------------------------------|
| —CF <sub>3</sub>                   | 6                             |
| —CF <sub>2</sub> H                 | 15                            |
| —CF <sub>2</sub> —                 | 18                            |
| —CH <sub>3</sub> crystal           | 22                            |
| —CH <sub>3</sub> monolayer         | 24                            |
| —CH <sub>2</sub> —                 | 31                            |
| Poly(tetrafluoro ethylene) (PTFE)  | 18.5                          |
| Poly(ethylene) (PE)                | 31                            |
| Poly(ethylene terephthalate) (PET) | 43                            |

The practical issues surrounding these steps are discussed in more detail below. Progress in understanding morphological wetting transitions, which underlie CDC, has been recently reviewed by Lipowsky.<sup>10</sup>

### Application of the mask

The lyophobic mask, which defines the areas where the target solution will be deposited, can be created in a variety of ways. The minimum requirement is for a surface energy pattern that has sufficient contrast to ensure that liquid is moved from the regions of low surface energy onto the regions of high surface energy. For the majority of our work we have used flexographic printing, since this is a well-established low cost, high throughput, roll-to-roll patterning technique, able to deposit a wide range of solutions onto a wide range of support materials. The resolution of this and other conventional printing techniques is limited to a few tens of micrometers. A way of improving the resolution is to use the soft lithography approach first described by Whitesides and co-workers.<sup>11</sup> Various optical methods involving, for example, lasers to ablate or deposit material,<sup>3</sup> and optically-switchable materials that change their surface energy when exposed to UV light<sup>12</sup> have also been investigated.

### Coating the target liquid

Once the lyophobic mask has been created on the substrate, the next stage is to overcoat both the masked and unmasked areas with the target liquid. We have focused our work on continuous liquid film coating methods, in particular slide-hopper coating.<sup>13</sup> However, CDC is not limited to this technique. There are many other ways in which the target material may be applied. For example, we have demonstrated that gravure coating can also be used to deposit a uniform liquid layer on the masked substrate.

### Destabilizing the target liquid

Although it is energetically favorable for liquid to move from the lyophobic to the lyophilic regions, this will not always occur spontaneously, particularly if there is no free wetting line present. This is often the case for the relatively thick, uniform, continuous liquid layers produced by slide hopper coating, since the wetting line at the edge of the substrate may be pinned by the edge of the support. To make the liquid de-wet in the desired pattern, a free wetting line must be generated. Methods of achieving this are described in the experimental section.



**Figure 1. Schematic illustration of the successive steps involved in CDC.**

(a) Support masked with lyophobic pattern. (b) Over-coating of target liquid. (c) Dewetting of target liquid into lyophilic regions.

### Rate of retraction

The speed at which the target liquid dewets the mask is clearly important, since it limits the overall speed at which the CDC process can be accomplished and so impacts productivity and cost. Brouhard-Wyart and coworkers have studied the rate of retraction of liquid films from lyophobic surfaces.<sup>14</sup> Their expression for the rate of retraction based on a hydrodynamic analysis is

$$V_R = k \frac{\gamma_{LV} \theta^3}{\eta} \quad (2)$$

where  $\eta$  is the dynamic viscosity of the liquid,  $\theta$  its equilibrium contact angle (in radians), and  $k$  is a constant for a given system, which in their experiments ranged from 0.003 to 0.01. Experimental data obtained for aqueous glycerol solutions in our laboratory gave a value of  $\sim 0.007$ , which is consistent with the literature values. However, when other liquids were used, such good agreement was not always found. Nevertheless, Eq. 2 provides a useful guide to the direction in which the various key parameters should be adjusted in order to maximize  $V_R$ . Evidently, a high contact angle, high surface tension, and low viscosity are all beneficial. Such a conclusion also follows from an alternative theoretical treatment based on the concept of wetting-line friction.<sup>15</sup> Factors, such as surface roughness and chemical heterogeneity, should be avoided, since they lead to contact angle hysteresis and hence to contact line pinning and unsteady recession.<sup>16</sup> Using Eq. 2 with  $k = 0.007$  and appropriate values of  $\gamma_{LV}$ ,  $\eta$ , and  $\theta$ , the retraction rate for water on a fluoropolymer is estimated to be more than  $300 \text{ cm s}^{-1}$ . For a  $10 \text{ mPa s}$  aqueous solution having a surface tension of  $40 \text{ mN m}^{-1}$  dewetting the same surface, the figure falls to about  $10 \text{ cm s}^{-1}$ .

## Experimental Methods

### Flexographic printing

Our initial attempts at creating lyophobic mask patterns involved using a hand-proofing device, the Esiproof, supplied by RK Print Coat Instruments, Royston, UK.<sup>17</sup> Using a rubber roller engraved with  $15 \times 30 \text{ mm}^2$  rectangles, it was possible to print a test pattern of lyophobic mask material. The masks could then be over-coated with the target solution using a manually operated blade coater. With this methodology we were able to investigate the effects of a wide range of mask materials and solution parameters (e.g. surface tension, viscosity, temperature, and layer thickness) on the rate and efficiency of liquid retraction, without the need for large quantities of materials.

At a later stage in the development of the method we used a Rotary Koater, a pilot-scale, flexographic printer also supplied by RK Print Coat Instruments, Royston, UK. The photopolymer material for the flexographic plates was supplied by Asahi, Japan, and the plates were obtained from Advance Graphics, Watford, and MPH Ltd., Harwich. Before using the Rotary Koater to print lyophobic masks, the operating parameters were optimized to ensure the best print quality.

### Coating the target liquid

For preliminary and various screening experiments a K-coater manual coating device was used (RK Print Coat Instruments Ltd, Royston, UK<sup>17</sup>). We found that the K-coater gave a good indication of whether or not a particular solution could be patterned using the CDC method. However, the majority of coatings were made using a pilot-scale, roll-to-roll coating machine at the Kodak facility in Harrow, UK.

For the pilot-scale coatings we used a 10.2-cm wide slide coating die to deposit the target liquid. The substrate was conveyed through the coating station, a cooled chill-box, and heated drying cabinets at a typical speed of  $8 \text{ m min}^{-1}$ . The driers were set using standard guidelines, bearing in mind that the wet thickness to be dried in the unmasked areas would be augmented by the liquid displaced from the masked areas. The suction was set low, just above break-line conditions ( $50\text{--}100 \text{ Pa}$ ).<sup>13</sup> This provided a slight destabilizing effect that triggered onset of film rupture and recession.

### Destabilizing the coated layer

When coating relatively thick (i.e.  $>1 \text{ }\mu\text{m}$ ) layers, rupture of the liquid leading to recession onto the lyophilic areas may or may not occur spontaneously, dependent on the mask pattern. For instance, if the pattern has lyophilic regions along the edges of the support, then the liquid may be pinned at the edge, despite the presence of lyophobic regions beneath the liquid layer. Spontaneous rupture of the liquid over the lyophobic regions will occur only if the liquid layer is locally thin enough for long-range intermolecular forces to dominate, say,  $100 \text{ nm}$  or less. Conversely, if the pattern has lyophobic regions along the edges of the support, then this will prevent pinning, and the wetting line will spontaneously move inwards as the liquid withdraws from the masked areas. However, layers that destabilize in this manner tend to yield thicker coatings towards the center of the web. If a uniform distribution of the target liquid over the entire pattern is to be obtained from a uniform over-coated liquid layer, then the layer must be destabilized at regular intervals.

An air-bar destabilizer device was therefore constructed to create holes in the liquid layer, at equal intervals across the coated width. The destabilizer consisted of 18 nozzles connected to a compressed air supply of ~70 kPa via a distribution manifold. An array of solenoid valves allowed the airflow through each nozzle to be pulsed in a regular manner. The solenoids were driven by an 18 V peak-to-peak, sine wave from an arbitrary function generator, TTI Corp. This enabled the frequency of the air pulses to be adjusted to produce holes coincident with lyophobic regions in the mask pattern.

## Materials

### Lyophobic mask

The principal lyophobic mask materials used in this study were FluoroPel PFC 604A and FluoroPel 804A, both supplied by the Cytonix Corporation (Beltsville, MD 20705, USA). These are 4% solutions of the same fluoropolymer in a fluorosolvent. For the FluoroPel PFC 604A, the solvent is HFE 7100 (3M Company), boiling point 61°C. With the FluoroPel PFC 804A, a higher boiling point fluorosolvent (84°C) is used. Mask materials were initially screened by measuring the advancing contact angle of water on test coatings made using the Esiproof, hand-proofing device. The best materials were later flexographically printed using the Rotary Koater. The angles were measured for microliter-sized water drops using a FIBRO DAT 1100 (FIBRO System AB, Stockholm, Sweden).

Of the materials tested, four gave advancing contact angles for water greater than 100°: the two fluoropolymers supplied by Cytonix (FluoroPel PFC 604A and PFC 804A), Modiper F600 supplied by the NOF Corporation, and Dow Corning's Z-6689. The values obtained for all these materials were very similar and lay in the range 107–120°, as shown in Table 2.

On the basis of the contact angles, there was little variation in the lyophobicity of the four surfaces. However, advancing contact angles do not necessarily give a good indication of the dewetting behavior of a liquid from a given surface; a parameter more representative of this behavior is the maximum speed of dewetting. Final ranking of mask materials was therefore carried out by directly measuring the rate of retraction of aqueous glycerol solutions from the test coatings using a method based on the work of Podgorski et al.<sup>18</sup> Table 2 shows that the Cytonix materials both had a significantly higher maximum dewetting speeds for 84% w/w aqueous glycerol solutions, which indicates greater suitability for CDC.

### Substrate

The substrate was a continuous web of 100 µm thick poly(ethylene terephthalate) (PET) with a thin (<1 µm) gelatin subbing layer (Kodak Limited, UK). The subbing layer has been optimized over many years to ensure good coatability and adhesion for aqueous solutions, and is characterized by a moderately high static advancing contact angle (with respect to water) but a zero receding angle. The latter ensures that the receding wetting line stays pinned on the target areas. If other supports are used, the surface properties must be optimized similarly to obtain good coatability and adhesion.

**Table 2. Maximum Speed of Dewetting of 84% w/w Aqueous Glycerol Solution, and Advancing Contact Angle of Water on PET Treated With Four Different Lyophobic Materials**

| Mask Material                       | Maximum Speed of Dewetting (mm s <sup>-1</sup> ) | Advancing Water Contact Angle (Degrees) |
|-------------------------------------|--|---|
| Cytonix PFC 604A                    | 54   | 120                                     |
| Cytonix PFC 804A                    | 49   | 113                                     |
| Dow Corning: Z-6689 Water Repellent | 8  | 107                                     |
| NOF Corporation: Modiper F600       | 36   | 113                                     |

### Coating materials

Gelatin, Type IV de-ionized, alkali processed, ossein derived gelatin, Eastman Gelatin. Glycerol, Sigma-Aldrich. Poly(vinyl pyrrolidone) (PVP) (360,000 Da), GAF. Poly(vinyl alcohol) (PVA), GH17, Goshen. Poly(3,4-ethylenedioxythiophene) poly(styrenesulfonate), (Baytron P), HC Stark. Organic solvents, methanol, toluene, and cyclopentanone, Sigma-Aldrich. Aqueous blue dye (4-(4,5-dihydro-4-(5-(5-hydroxy-3-methyl-1-(4-sulfophenyl)-1H-pyrazol-4-yl)-2,4-pentadienylidene)-3-methyl-5-oxo-1H-pyrazol-1-yl)benzenesulfonic acid), Eastman Kodak Company.

### Nonionic surfactants

10G (nonyl phenoxy poly(glycidol)(10)), Olin Corporation. Triton X100 (TX100) (iso-octyl phenoxy polyethoxyl (9-10) ethanol), Sigma-Aldrich. Acrylamide surfactants C<sub>12</sub>H<sub>25</sub>-S(A)<sub>10</sub>H and C<sub>8</sub>F<sub>17</sub>(CH<sub>2</sub>)S(A)<sub>13</sub>H, and sugar surfactant C<sub>6</sub>H<sub>13</sub> bis-gluconamide (C<sub>6</sub>H<sub>13</sub>)<sub>2</sub>C(CH<sub>2</sub>NHCO(CHOH)<sub>4</sub>CH<sub>2</sub>-OH)<sub>2</sub>, Eastman Kodak Company. Saponin, Sigma-Aldrich.

### Anionic surfactants

Aerosol OT (AOT) and Sodium dodecyl sulphate (SDS), Sigma-Aldrich. Triton X200E (TX200E) (ethanesulfonic acid, 2-(2-(2-(4-(1,1,3,3-tetramethylbutyl) phenoxy)ethoxy)ethoxy)-sodium salt), Eastman Kodak Company. Alkanol XC (sodium alkyl naphthalene sulfonate), DuPont. All materials were used as supplied.

## Results and Discussion

In the previous sections we described the various steps involved in the CDC method: application of the lyophobic mask; over-coating with the target solution; destabilizing the liquid film; and drying/curing the patterned layer.

The schematic in Figure 2 illustrates the coating and destabilization steps. Here, an aqueous target solution (6% w/w gelatin, 0.1% w/w blue dye, 0.01% w/w 10G surfactant) is being coated at 8 m min<sup>-1</sup> on the pilot-scale coating machine. The PET substrate has been preprinted with a lyophobic mask of FluoroPel PFC 604A using the Rotary Koater. After coating, the target solution retracts rapidly from the mask and collects on the lyophilic unmasked areas, in this case 15 × 30 mm<sup>2</sup> rectangles. The conical nozzles of a prototype air-bar stabilizer can be seen in the top of the picture; however, the device is not in use. The coating is therefore unstable only at the edges of the mask, and the liquid retracts inwards towards the center of the web, revealing

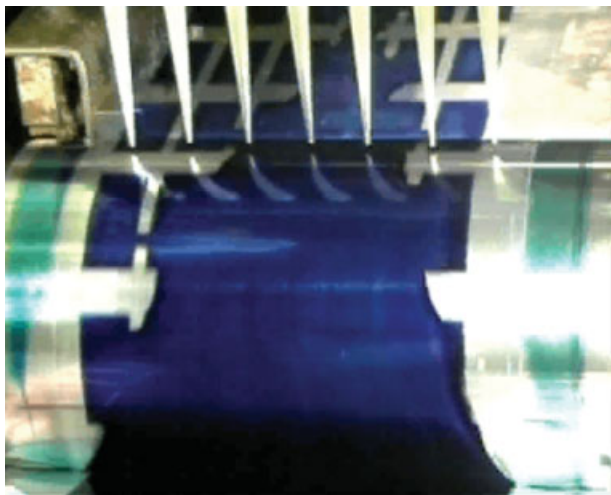


**Figure 2. Pilot-scale coating of a blue target solution over a masked PET substrate.**

The solution is deposited from a slide coating die (at the bottom of the picture) as the substrate passes over a coating roller. A V-shaped receding wetting line can be seen as the liquid de-wets from the edges of the substrate, revealing a pattern of  $15 \times 30$  mm coated cells. The conical nozzles of a prototype air-bar establisher device (not in use) can be seen at the top of the picture. A color video of the process is available in the Supplementary Information. [Color figure can be viewed in the online issue, which is available at [www.interscience.wiley.com](http://www.interscience.wiley.com).]

the rectangular coated cells as the substrate is conveyed towards the chill-box and drier. The characteristic V-shaped appearance of the receding wetting line<sup>19</sup> is clearly visible in the picture. A video sequence of the process is available as supplementary information.

### Characteristics of the target solution

**Functional Materials.** For the majority of this study, the target solutions were based on gelatin (Type IV de-ionized, alkali processed, ossein derived gelatin, Eastman Gelatin) as it is readily available and has good coating qualities. In addition, its solutions can be chill-set immediately after coating. This helps to pin the liquid at the edges of the coated areas, preventing further withdrawal and the appearance of defects. Pinning has important implications for the sharpness of the coated edges and will be discussed in more detail below.

We also used CDC to pattern the following functional materials: aqueous solutions of glycerol (CAS no. 56-81-5) and polymers such as PVP (CAS no. 009003-39-8), and PVA (GH17, CAS no. 25213-24-5); photonic crystals (monodisperse PMMA/BA, a gift from University of Bristol); conductive organic materials such as PEDOT (Baytron P, HC Stark); and mixtures of organic solvents. We did not identify a general category of materials that could not be patterned. However, for each target solution, it was necessary to optimize the viscosity and surface tension. As shown by Eq. 2, the rate of retraction of the target solution from a given mask surface can be increased by maximizing the surface tension of the solution and by minimizing its viscosity.

**Surface Tension and Surfactant Effects.** For solutions with intrinsically low surface tensions, the retraction rates are likely to be low. Nevertheless, we found that the CDC

method could still be used to pattern coat a solvent mixture comprising 72% w/w toluene, 23% w/w methanol, and 5% w/w, and having a surface tension as low as  $20 \text{ mN m}^{-1}$ .

With gelatin-based solutions, the situation was more complex. In the absence of any surfactant, the retraction rate from the masked areas was impracticably slow and could be variable, even though the surface tension of the solution was moderately high ( $\sim 60.5 \text{ mN m}^{-1}$ ). Viewed under an optical microscope, the wetting line of a sessile drop of a dilute gelatin solution was found withdraw with an unsteady “stick-slip” motion as liquid was removed. Interestingly, this behavior was not observed when target solutions based on glycerol, PVP, or PVA were used, even though these had similar surface tensions and viscosities. To investigate the effect, sections of the printed mask were examined using Normarski interference microscopy. A typical image (Figure 3a) shows that the uniformity of the mask could be quite poor. This was true whether the mask was printed by hand or by machine. In both cases, there appeared to be areas where the coverage of fluoropolymer was not complete. Gaps or pinholes in the mask would allow the gelatin solution to interact with the underlying gelatin-based subbing layer, thereby creating points at which the wetting line could become pinned.

A Normarski interference micrograph taken of a sample of subbed PET dip-coated with FluoroPel PFC 804A is shown in Figure 3b. Clearly, the dip-coated sample is much more uniform than the printed sample and, as a consequence, gave more uniform solution retraction.

Experimentation showed that the problem with the printed masks could be overcome by judicious use of surfactants. In particular, we found that when the surfactant 10G was added at a low level (0.01% w/w), the solution retracted rapidly from the printed mask and partitioned completely onto the lyophilic areas. No stick-slip behavior was observed. A working hypothesis is that the gaps and pinholes in the mask allow the 10G surfactant to adsorb on the exposed surface of the gelatin-subbing layer with their lyophobic groups directed towards the solution, thus reducing the interaction. Increasing the concentration of the 10G to 0.1% w/w resulted in a slightly slower retraction rate, but partition of the liquid was still completed within 10 s. A further increase in concentration to 1.0% w/w gave a similar result, but with no further reduction in retraction rate. This can be understood in terms of Eq. 2, since the surfactant has negligible effect on the viscosity of the solutions, and the surface tension of the 0.1% and 1% solutions were the same ( $\sim 31 \text{ mN m}^{-1}$  at  $40^\circ\text{C}$ ), but lower than that of the 0.01% solution ( $43.9 \text{ mN m}^{-1}$ ). We therefore conclude that while a low concentration of 10G is beneficial in overcoming the stick-slip behavior, further additions slow retraction through the reduction in surface tension.

10G is a fairly typical nonionic surfactant, and we found that other nonionic surfactants were also beneficial when used at low concentrations. For example TX100 at 0.01 and 0.1% w/w, acrylamide surfactants  $\text{C}_{12}\text{H}_{25}\text{S(A)}_{10}\text{H}$  and  $\text{C}_8\text{F}_{17}(\text{CH}_2)\text{S(A)}_{13}\text{H}$  at 0.1% w/w, and sugar surfactant di- $\text{C}_6\text{H}_{13}$  bis-gluconamide at 0.05% w/w were investigated in 6% w/w gelatin solutions. In all cases, the solutions retracted uniformly from the printed mask and partitioned completely onto the lyophilic areas.

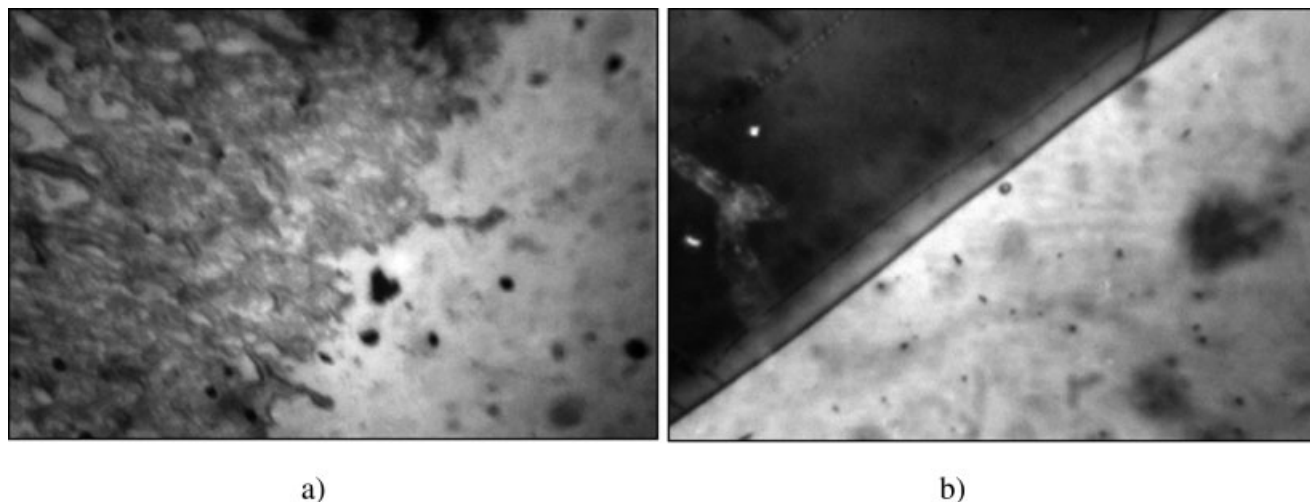


**Figure 3. Normarski interference micrographs of the lyophobic mask.**

(a) Mask printed with FluoroPel PFC 804A using the Esiproof device. The masked area appears darker than the adjacent unmasked area.  
 (b) Mask dip-coated in the FluoroPel PFC 804A solution, the masked area appears darker than the adjacent unmasked area.

Some anionic surfactants also proved effective in gelatin solutions. TX200E at 0.1% w/w and SDS at 0.01 and 0.1% w/w induced rapid retraction. However, comparable improvements were not found with other anionic surfactants such as AOT at 0.003, 0.01, and 0.03% w/w, and Alkanol XC at 0.01 and 0.1% w/w, or with the natural nonionic surfactant Saponin at 0.1%. In the case of the Saponin, there was little or no retraction of the coating solution from the lyophobic areas. Saponin is known to be a film forming material as a result of its high surface viscosity rather than any great ability to lower surface tension,<sup>20</sup> and it is presumably this high surface viscosity that inhibits retraction.

With the AOT and the Alkanol XC solutions, the liquid retracted completely from the lyophobic mask at the lower concentrations, but at the higher concentrations the retraction was significantly slower and did not proceed to completion. There are at least two factors that may explain these differences. First, although the surface tensions of the anionic surfactant solutions are comparable to those of the nonionic surfactants, the viscosities may be very different. With anionic surfactants, the viscosity of gelatin solutions increases steeply with increasing concentration once the critical aggregation concentration (CAC) of the surfactant is reached. This is due to interaction between the surfactant micelles and the gelatin strands.<sup>21</sup> The increased viscosity will reduce the rate at which the liquid can retract from the mask. Second, it is widely accepted that the organization of surfactants like AOT adsorbed at a lyophilic surface can change with increasing concentration from being a monolayer with the lyophobic group directed towards the solution to a bi-layer structure with the lyophilic groups of the second layer outermost.<sup>22</sup> The exact concentration at which this occurs is related to the critical micelle concentration (CMC) of the surfactant, which for AOT is at about 0.2% w/w<sup>23</sup> and for Alkanol XC at about 0.1% w/w. If such a bi-layer were to be formed at the substrate surface via the gaps in the printed mask, the lyophilic groups would act as pinning points to inhibit retraction of the coated liquid in the same way as the initial gelatin subbing layer.

*Limiting Viscosity of Target Solutions.* To investigate the upper solution viscosity limit for the CDC process, a series of experiments was conducted with two non-gelling polymers, PVP and PVA, at various concentrations (1–10% w/w). The solutions were coated at three wet thicknesses (50, 100, and 150  $\mu\text{m}$ ) in order of increasing concentration, and the rate of retraction from the masked areas was investigated.

In the case of the PVA solutions, at 7% w/w (143 mPa s at 23°C), the retraction rate was very slow ( $<10 \text{ mm s}^{-1}$ ) at a thickness of 50  $\mu\text{m}$  and was incomplete at the highest lay-down. However, with the PVP solutions, reasonable retraction rates ( $>10 \text{ mm s}^{-1}$ ) were obtained even at 10% w/w (295 mPa s at 23°C) at all three wet thicknesses. Thus, the exact upper solution viscosity limit for coating appears to be dependent upon the target liquid. Following the same arguments as advanced for the behavior of gelatin solutions, we suggest that retraction efficiency in the case of the polymers also depends upon whether or not the solution interacts with the underlying subbing layer through gaps and pinholes in the printed mask. For target solutions where these interactions are likely to be negligible or where mask quality can be improved, our results suggest that solutions with viscosities up to at least 300 mPa s could be pattern coated. However, in practice, the upper viscosity limit for a continuous process will also depend on the coating method. For example, the useful range for single-layer slide coating is from a few mPa s up to a few tens of mPa s. And while methods such as slot, blade, or dip coating can be used for more viscous liquids, the retraction rate must still be fast enough to make continuous roll-to-roll coating a practical proposition.

### *Cell Geometry, topology, and orientation*

Figure 4a shows a test pattern designed to investigate the influence of coated cell geometry (shape, size, pitch), topology, and orientation on the effectiveness of CDC. Figure 4b shows the result obtained when gelatin-subbed PET, flexographically printed with a mask of the pattern shown in Figure 4a, was subsequently over-coated with a solution of 6%

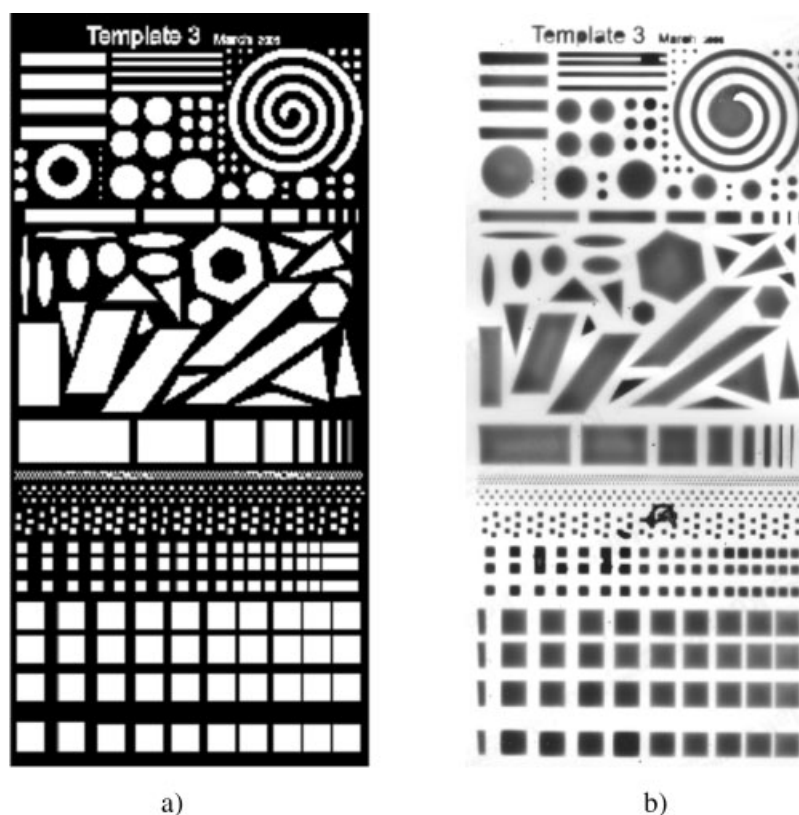


**Figure 4. (a) Test pattern designed to explore the geometry, topology and orientation of the cell shapes that can be coated using the CDC method; (b) the resulting coating after chilling and drying.**

For (a): the overall size of the pattern is  $130 \times 275$  mm; the smallest square regions are  $0.5$  mm. This test pattern was converted into a flexographic plate and a lyophobic mask was printed onto gelatin-subbed PET using the Rotary Koater. This was then over-coated on the pilot-scale slide coating machine with a solution of 6% w/w gelatin, 0.1% w/w blue dye and 0.01% w/w 10G at  $60 \mu\text{m}$  wet thickness.

w/w gelatin, 0.1% w/w blue dye and 0.01% w/w 10G at a wet thickness of  $60 \mu\text{m}$ . The result demonstrates the flexibility of the CDC method. Evidently, a wide range of cell shapes and sizes can be coated, irrespective of their orientation. Only three features in the test pattern failed to coat successfully: the spiral and the two concentric “donut-shaped” structures. In the former case, the wetting line initially moved around the spiral, but was eventually forced to stop, as there was no route whereby the liquid at the center of the spiral could escape. With the concentric structures, without a wetting line at the center, there was no path or mechanism by which the liquid could retract. Nevertheless, for both topologies, it was found that complete retraction of the liquid could be achieved if the liquid was destabilized at the center of the structures using a device such as the air-bar destabilizer described earlier.

### Resolution

The spatial resolution of the CDC method is determined largely by the resolution at which the lyophobic mask can be applied, but factors such as the thickness of the coated layer and the method by which the target liquid is coated also play an important role. Since the aim of the method is for all the target liquid to be deposited in the designated cells, these cells must be of sufficient area to accept all the liquid.

Using the Rotary Koater flexographic printing device we have found that it is possible to print lines as narrow as  $50 \mu\text{m}$ . Further work would, however, be needed to create features of this size on a regular basis. One of the limiting factors is the material used to fabricate the printing plate. Where this is not optimized for high-resolution printing, it is very difficult to obtain raised areas on the plate  $50 \mu\text{m}$  wide or less without these areas becoming distorted and irregular. A second factor is the pressure applied between the printing plate and the substrate, too high and the plate becomes deformed, too low and ink transfer is reduced. In addition, by controlling the fluidity of the mask solution and the amount of solution that was transferred from the plate to the substrate, it was possible to limit post-printing flow and so enable smaller features to be generated. Such an approach has been successfully applied in the area of soft lithography.<sup>11</sup> Higher resolution masks can also be made by other techniques such as optical writing methods.

Using the Rotary Koater to print the fluoropolymer mask followed by hand coating the target liquid we have demonstrated that it is possible, on a routine basis, (i) to coat lines down to  $100 \mu\text{m}$ , and (ii) to generate gaps down to  $50 \mu\text{m}$  for a coated wet thickness of  $20 \mu\text{m}$ . Experiments where the total wet thickness was increased to  $30 \mu\text{m}$  proved unsuccessful with such small features. When the coated layer was thicker, retraction of the liquid could be improved if the

coating were destabilized with the air-bar device, but retraction still did not proceed to completion, since there was nowhere for the excess liquid to go. The problem could be managed by creating a “picture frame” around the region of interest that acted as a drain to collect the surplus. This approach is described in more detail later.

### Coating uniformity

In assessing coating uniformity, the first step was to identify a suitable technique. It proved difficult to obtain a direct measurement of the coating thickness using standard profilometry, since the coatings were too compliant to avoid deformation by the stylus. Furthermore, the coated area was too large to make noncontact techniques such as white-light interferometry a practical alternative. Coating uniformity, both within the cells of our test pattern and across the width of the substrate, was therefore quantified by incorporating colored dyes in the coating solutions. Scanned images of the resulting coatings were then analyzed on the assumption that coating thickness was roughly proportional to image density. Analysis comprised the following steps: the dried coatings were scanned at 200 dpi using an HP Scanjet 5500c scanner; the scanned images were converted to a greyscale and the images reversed; finally, the line profiles of the greyscale pixel-values across each individual patch and across the full width of the coating were determined. The procedure is illustrated in Figure 5, which shows the results obtained for a pilot-scale coating of 6% w/w gelatin with 0.1% w/w blue dye at 57  $\mu\text{m}$  wet lay-down on a substrate masked to give multiple rectangular cells. The pattern was coated at 16  $\text{m min}^{-1}$ .

It is clear from the images in Figure 5 that almost all the cells show a region of lower density, i.e. lower coating thickness, at their centers, with a rounded capillary ridge or bead around the edge of each of cell. Such ridges are a common problem when coating within the width of the substrate, and arise at least partly as a result of the conflicting interfacial

curvature demands of a thin flat film terminating in a fairly large contact angle.<sup>24</sup> The width of the ridge depends on the surface tension and is commensurate with the capillary length. For the target solution used here, this length is of order 2–3 mm.

If we exclude the edge region, the percentage variation in uniformity within the cells in Figure 5 is about 25%. This is calculated by dividing the difference between the maximum and minimum mean greyscale values by the minimum value. In addition, the central cells are darker and therefore have a higher lay-down than the outer cells. This is because in these coatings, destabilization started at the edges and the flow of liquid was towards the center.

Various strategies for minimizing edge effects and improving both within-cell and cross-width uniformity are discussed below.

*Effect of Surfactant Concentration and Coating Thickness.* In the initial coating experiment shown in Figure 5, there was no surfactant present in the target solution. When the nonionic surfactant 10G was added at 0.01% w/w, a definite improvement in cell uniformity was observed. The improvement is presumably due to the reduction in surface tension (from 60.5 to 43.9  $\text{mN m}^{-1}$ ) and a concomitant reduction in the final contact angle, leading to better matching of edge curvatures to the coated thickness.<sup>25</sup> On the basis of the experience in conventional coating,<sup>25</sup> increasing the 10G to 0.1% should have given a further improvement; however, the resulting lower surface tension greatly reduced the rate at which the liquid retracted from the masked regions, rendering this option impractical.

The effect of increasing coating thickness on the overall uniformity was also investigated. When a solution of 6% w/w gelatin, 0.1% w/w blue dye, and 0.01% w/w 10G was coated at 100  $\mu\text{m}$ , the lay-down was approximately constant over the whole width of the cell. Unlike the cells coated in the initial experiment, there was no dip in thickness at the center (see Figure 8a). The combination of increased cover-

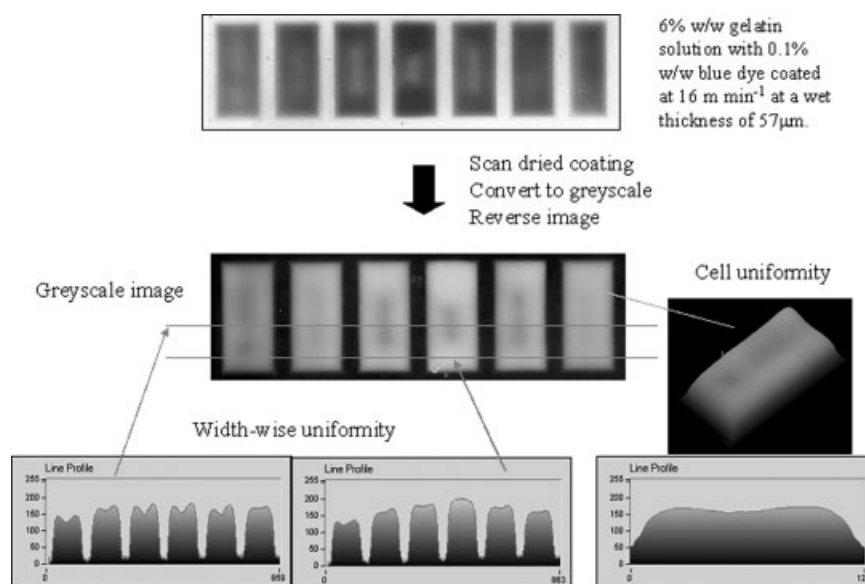


Figure 5. Image analysis method used to quantify the coating uniformity obtained with the CDC method.

age and 10G surfactant flattened the capillary ridge and reduced the variability in the coating thickness within the cell to about 2.5%, i.e. an order of magnitude lower than that obtained originally. Thus it seems likely that by judiciously manipulating solids content, coating thickness and surfactant concentration, it should be possible to produce patterned coatings using the CDC technique to a high degree of uniformity.

**Effect of Chill-Setting.** In our initial experiments, the chill-box on the pilot-scale coater was set at the highest practical temperature of 39°C in order to maximize the time available for the coating solution to retract. However, subsequent experiments showed that for gelatin-based target solutions, retraction was complete within a few seconds, allowing the chill-box temperature to be lowered. One benefit of this was that the sharpness of the cell edges was significantly improved.

A series of experiments were conducted in which the chill-box temperature was set at 4, 8, 16, and 39°C, with all other parameters kept the same. As before, the dried coatings were scanned and the greyscale values were plotted as a function of position across the width of each cell. With the chill-box temperature set at 39°C, we found that the coated solution tended to withdraw slightly from the edges of the cell during drying. This gave rise to a more gradual edge profile. At 16°C and below, gelation started immediately the coating entered the chill-box, pinning the solution at the edges of the cell. As a result, there was less withdrawal during drying and the edge profile was sharper.

For polymer solutions such as PVP and PVA that do not gel, an alternative strategy was developed. When a solution of 5% w/w PVA was coated at 150  $\mu\text{m}$  and 23°C, a significant reduction in the degree to which the solution withdrew from the edge of the cell during drying was observed on the addition of 0.1% w/w 10G (compare Figures 6a, b). However, to obtain sharp edges with this system it was also found necessary to add a volatile solvent. The more volatile solvent evaporates rapidly leaving a viscous, more concentrated solution of the PVA in the less volatile solvent that effectively becomes pinned at the cell edges. In the example shown in

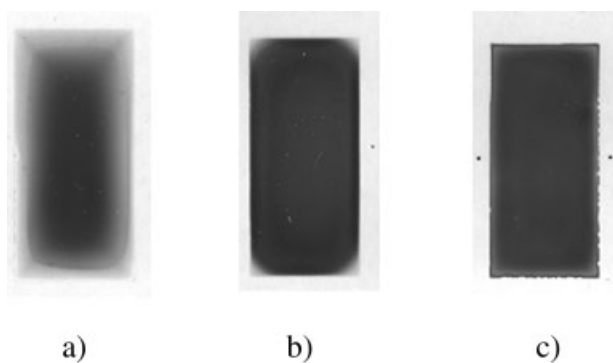


**Figure 6. Rectangular cells hand-coated with 150  $\mu\text{m}$  PVA solutions at 23°C.**

(a) 5% w/w PVA. (b) 5% w/w PVA with 0.1% w/w 10G. (c) 5% w/w PVA with 0.1% w/w 10G in a 50% w/w ethanol-water mixture.

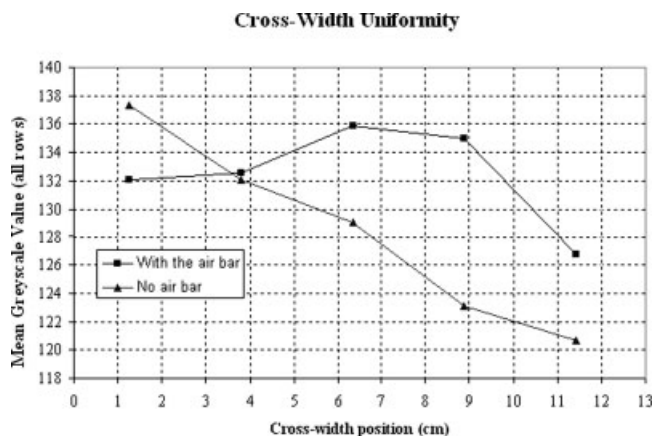


**Figure 7. Variation in cross-width uniformity obtained for 6% w/w gelatin, 0.1% w/w blue dye, and 0.01% 10G, coated as a 100  $\mu\text{m}$  layer at 8  $\text{m min}^{-1}$ , both with and without the use of the air-bar de-stabilizer.**

Figure 6c, the PVA was dissolved in a 50% w/w mixture of ethanol and water.

**Effect of Air-Bar Destabilizer.** We have already seen that the target solution is not always distributed evenly across the width of the substrate. The result depends not only on retraction rate and mask geometry, but also on the points of initiation and the resulting pathways. In the example given in Figure 5, the lay-down in the central cells is higher than in any of the outside cells, since retraction was initiated at the edges of the substrate and moved inward towards the center. In another example, where retraction started at one edge only, final lay-down was low in the cells on that side and gradually increased towards the other side. This asymmetric distribution is plotted in Figure 7. The graph refers to a coating of multiple rows of rectangular cells similar to those shown in Figure 5. The mean greyscale value for each cell (including the edges), averaged over six rows, is plotted as a function of the cross-width position. The variability in the cross width uniformity, calculated as before, is ~13.5%. This figure provides an estimate of the maximum variability that can be expected for this target solution, under the coating conditions used.

With the air-bar destabilizer in operation, retraction could be initiated at multiple points across the coating width. Using this approach the width-wise variability of a solution of 6% w/w gelatin, 0.1% w/w blue dye and 0.01% 10G was reduced to about 7%, as also shown in Figure 8. The combined benefits of surfactant, increased coating thickness and the air-bar destabilizer are illustrated in Figure 8.

In principle the lateral spacing (pitch) and frequency of the air pulses through the air-bar nozzles can be adjusted so that retraction is initiated at points coincident with the masked areas. To prevent liquid becoming isolated on masked areas, there should be only one point of initiation in each area.

**Effect of Pattern Geometry and Fluid Management.** Ideally, masks should be designed to facilitate destabilization and provide an efficient pathway for liquid retraction. We have already seen the problem presented by structures such

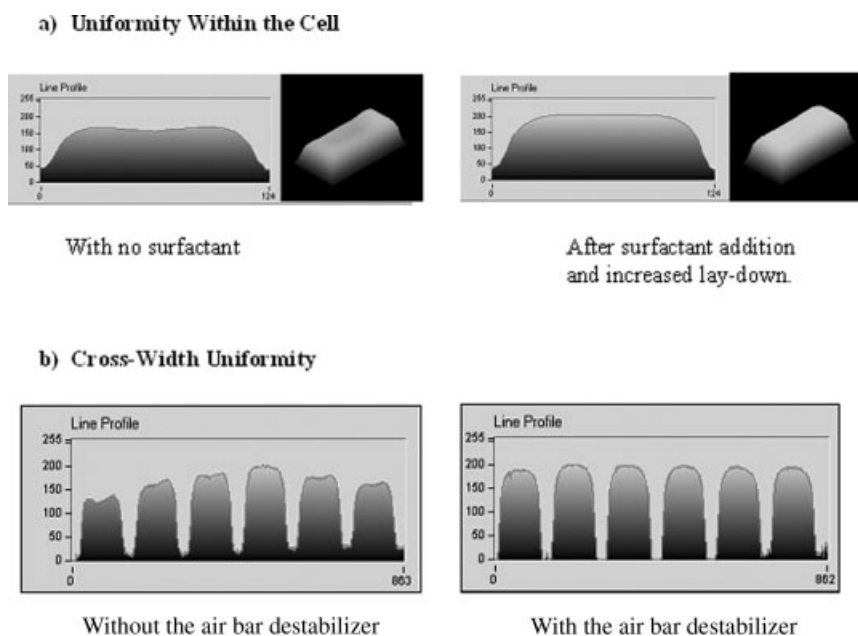


**Figure 8. Summary of the within-cell and the cross-width uniformity.**

Obtained when gelatin based solutions were coated on the pilot-scale coater at  $8 \text{ m min}^{-1}$ , showing the combined benefits of (a) surfactant addition and increased lay-down, and (b) the further use of air-bar destabilization.

as spirals and concentric patterns. However, there is a more general problem. If the proportion of coated to uncoated area is low, there may be excess target solution and nowhere for it to go. The problem will get progressively worse as the proportion of coated area goes down and the wet lay-down goes up. In such circumstances, it is important to develop strategies for managing the excess liquid. One simple approach is to create a lyophilic border that frames the patterned area and collects the surplus. Such an approach has been tested using the printing plates illustrated in Figures 9a c. Lengths of substrate printed with this lyophobic mask pattern were subsequently over-coated with the usual test solution of 6% w/w gelatin, 0.1% w/w blue dye and 0.01% w/w 10G. The resulting coatings, shown without (Figures 9b) and with the lyophilic border present (Figure 9d), demonstrate that the uniformity of the coatings is significantly improved by providing a sink for the excess liquid. Addition of the lyophilic border allows the excess liquid at the edges of the coating to be collected, instead of being deposited into the cells around the edges of the grid of squares. The cross-width variability (across the entire matrix, including the edges) is about 10% with the lyophilic border as compared to 22% without.

The spacing between the cells is also important in delivering coating uniformity. As the size of the lyophobic areas increases, the amount of liquid that must be displaced and the distance over which it must be transported both increase. Thus, further enhancements in coated uniformity should be possible by minimizing the gaps between the cells. In addition, minimization of the gaps will increase the overall rate at which CDC can be carried out. This rate will depend in a complex way, not only on the dewetting speed, but also upon the distance over which dewetting must occur, the direction of dewetting, and the number of dewetting fronts. By careful design of the mask and suitable destabilization procedures, overall process speeds can be significantly greater than the underlying speed of dewetting.

### Coating thickness

The wet thickness of the layer that can be applied by CDC is largely dependent upon the method used to coat the target solution. All coating methods, including slide coating, curtain coating, roll, blade or air knife coating, gravure coating, ink-jet, and electro-spray, work most effectively within a specific range of wet thicknesses. This range will influence the method selected for a given application.

In our work, we have mainly used slide coating where the accessible range of wet thicknesses is typically about  $5\text{--}150 \mu\text{m}$ . The exact values are governed by process parameters such as coating speed, solution viscosity and suction. At the upper end of this range, liquid retraction from the mask may not be spontaneous, and a device to initiate retraction, such as the air-bar destabilizer, will be beneficial. At the other extreme, in order to deposit layers thinner than about  $5 \mu\text{m}$ , an alternative coating method must be considered. Here, we have demonstrated the feasibility of depositing nonaqueous solvent-based liquids with a wet thickness of a few micrometers using a gravure printer.

Coating thickness will also depend upon the resolution demands of the pattern. For a small circular cell, the liquid will adopt spherical-cap geometry. The height of this cap will determine the maximum thickness obtainable. If we assume a hemispherical cap, the maximum height will be half the width of the drop. Thus, when patterning very fine lines, the thickness of the coating must be less than about half the line width, else the excess liquid will spill over, distorting the pattern.

The exact height of the liquid remaining within the cell will depend not only on the volume of liquid available, but also on the contact angle adopted at the edge of the cell. Because of contact-line pinning at the boundary between a lyophilic cell and the surrounding lyophobic mask, the contact angle is variable. Its maximum value is given by the static advancing contact angle of the liquid on the mask

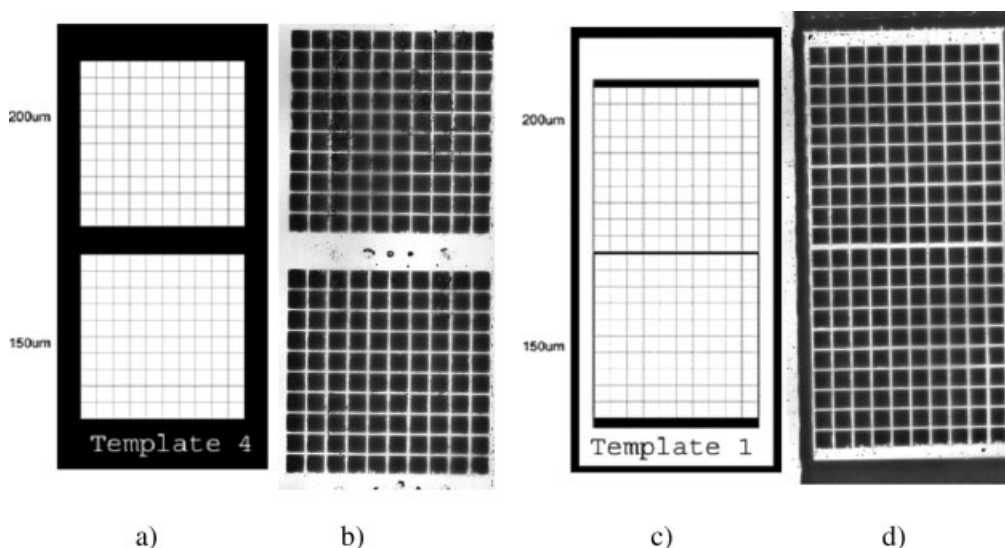


**Figure 9. Effective liquid management in the CDC process.**

This experiment was conducted using printing plates with an array of squares (a) and with the same array of squares surrounded by a lyophilic border to capture excess coating solution (c). The patterns obtained when a solution of 6% w/w gelatin, 0.1% w/w blue dye and 0.01% w/w 10G was coated as a 100  $\mu\text{m}$  layer at 8  $\text{m min}^{-1}$  are shown for the array of squares (b) and the array of squares surrounded by the lyophilic border (d). In (b) the cells at the edge of the array have a greater thickness compared to those in the center, in (d) the excess liquid has been captured around the edge of the array, resulting in a more uniform thickness throughout the entire array.

$\theta_{A, \text{Mask}}$ . Conversely, its minimum value is given by the receding angle on the lyophilic substrate, which is ideally zero. As the size of the cell increases, the maximum possible height for the drop will itself pass through a maximum before gravity begins to flatten the profile and the height eventually reaches a plateau value given by

$$h_{\text{max}} = \sqrt{\frac{2\gamma}{\rho g} (1 - \cos \theta)} \quad (3)$$

where  $\rho$  is the density of the liquid and  $g$  the acceleration due to gravity.<sup>26</sup> Since the angle at the edge of the cell can take any value between  $\theta_{A, \text{Mask}}$  and zero, all drop heights between that given by Eq. 3 with  $\theta = \theta_{A, \text{Mask}}$  and zero are potentially stable, provided the cell is sufficiently large. For water on a fluorocarbon surface  $h_{\text{max}}$  is about 4 mm, so for large cells high coating thicknesses should not present a problem.

The final dry thickness of the layer will, of course, depend upon the solids content of the solution coated. Thicker (or thinner) dry layers can be obtained by increasing (or decreasing) the percentage solids, but only within the limits imposed by the operability constraints of the coating method and the need to keep the viscosity and surface tension of the solution optimized for rapid retraction from the mask. Thicker dry coatings may also be obtained by successively coating additional layers using the same mask.

### Simultaneous multi-layer coatings

Thus far we have discussed the use of CDC to pattern coat only single layers. For many applications, however, it will be necessary to assemble multiple layers with either the same or different patterns. CDC uses differences in surface energy to direct the target solution. Once the process is complete, and

the solution is dried or cured, the lyophobic mask remains in place, substantially unaffected by its initial use. This is clearly beneficial for coating additional layers with the same pattern. If the sample is over-coated with a second target solution, the liquid will retract from the mask in exactly the same way as before, but this time collecting on top of the first dried layer – provided that layer is sufficiently lyophilic.

In principle, this approach could be used to build up multiple layers by repeatedly passing the dried sample through the coating machine, applying a single layer at each pass. However, multiple layers can be applied more efficiently by coating them simultaneously<sup>13</sup> with the same pattern in a single pass.

In order to investigate the feasibility of such a process, a series of two-layer coatings were made on the pilot coater, in which the thickness ratio of the layers, the surfactant levels (and hence the surface tensions) in both layers, and the viscosity of just the top layer were all varied. The two layers were applied using a standard two-slot slide coating die operating under conditions of laminar flow, which prevents mixing.<sup>13</sup> Figure 10 shows a two-layer coating successfully obtained by this method. Here, a top layer consisting of 13% w/w gelatin, 0.1% w/w aqueous blue dye, and 0.01% w/w 10G (wet thickness 10  $\mu\text{m}$ ) and a bottom layer of 6% w/w gelatin and 0.1% w/w aqueous yellow dye (wet thickness 90  $\mu\text{m}$ ) have been patterned simultaneously at 8  $\text{m min}^{-1}$ .

While Figure 10 demonstrates that good quality two-layer coatings can be achieved, our study showed that simultaneous two-layer coatings were not possible over the whole range of coating parameters. For example, to ensure that the top layer remained completely spread over the lower layer it was necessary to arrange that the surface tension of the top layer was always lower than that of the bottom. Such constraints are well known from conventional multilayer slide coating. In situations where this surface tension requirement

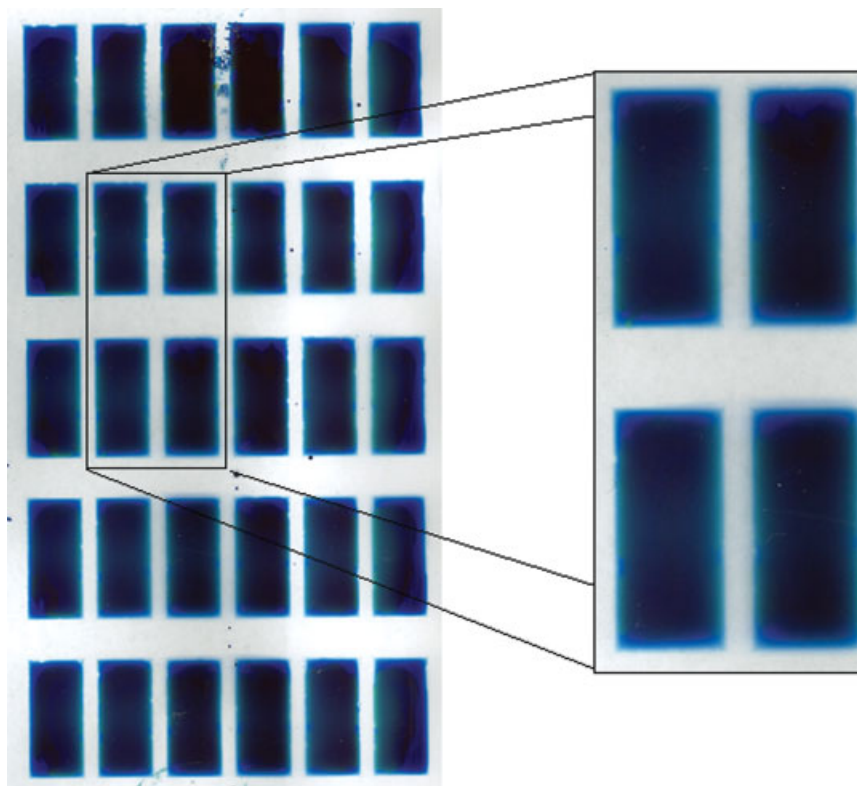


**Figure 10. Two-layer coating patterned simultaneously using the CDC method.**

The top layer is a solution of 13% w/w gelatin, 0.1% w/w blue dye and 0.01% w/w 10G coated at  $10\mu\text{m}$ . The bottom layer is a solution of 6% w/w gelatin and 0.1% w/w yellow dye coated at  $90\mu\text{m}$ . [Color figure can be viewed in the online issue, which is available at [www.interscience.wiley.com](http://www.interscience.wiley.com).]

is not met, edge withdrawal occurs on the slide immediately prior to coating and the different layers may become inter-mixed. Furthermore, to ensure that the retraction of the target solution from the mask was sufficiently fast, it was necessary to keep the total amount of surfactant present in the layers as low as possible. Best results were obtained when there was minimal surfactant in the top layer and either no surfactant or a lower level in the bottom layer.

Close examination of the uniformity around the edges of the cells in Figure 10 (see detail) shows that there is some withdrawal of the top layer relative to the bottom. By using a relatively viscous top layer, this effect could be minimized. However, we found that it was essential to keep the thickness of the top layer small relative to the bottom one in order to ensure complete retraction of the layers from the mask.

To investigate whether this multi-layer coating capability for CDC could be extended from two layers to three, further coating experiments were conducted. The following factors were investigated: the thickness ratio of the three layers; the thickness of the bottom layer; and the viscosity of the bottom layer. A simultaneous three-layer coating is shown in Figure 11. Best results were obtained when:

- (i) The top two layers were kept as thin as possible.
- (ii) The viscosity of the top layer was kept relatively high in order to ensure that any withdrawal of the coated liquid from the edges of the cells was minimized.
- (iii) The total amount of surfactant in the pack was kept as low as possible.

- (iv) The surfactant concentration was highest in the top layer with no surfactant in the bottom layer.

## Summary and Conclusions

We have demonstrated that CDC can be used to create discrete, coated areas on flexible support in a continuous roll-to-roll manner. The method, which utilizes differences in surface energy (wettability) to direct liquid into the required areas, is low cost and can be used to pattern a wide range of materials at potentially high speeds. Using flexography to print a fluoropolymer mask followed by slide coating of the target liquid, we have shown that it is possible to coat lines down to  $100\mu\text{m}$  and generate gaps down to  $50\mu\text{m}$ . Using alternative means to create the surface energy mask, such as micro-contact printing or optical techniques, it should be possible to create even finer features. The viscosity of the target solution that can be patterned is dictated initially by the method used to over-coat the surface energy pattern. For slide hopper coating this is in the range from a few mPa s up to the order of 100 mPa s. However, by using methods such as slot or blade or even dip coating, it is possible to pattern more viscous solutions of the order a few hundred mPa s. The limiting factor with very viscous liquids is the increased time it takes for the liquid to de-wet from the lyophobic mask.

CDC can be used to pattern relatively thick layers compared to other technologies. In our work, we have used slide

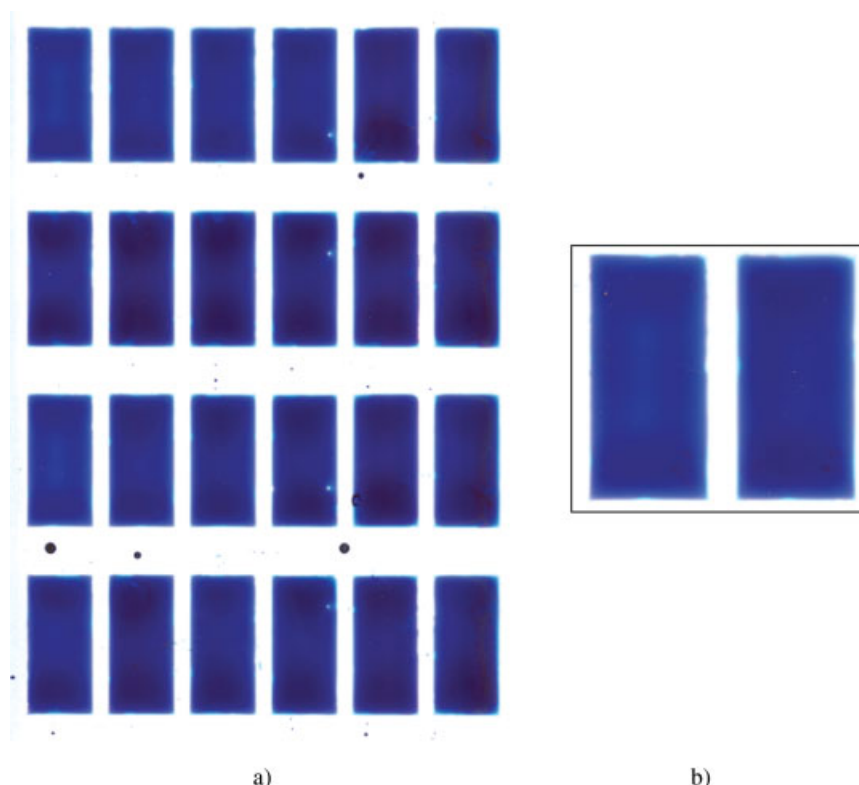


**Figure 11. Three-layer coating patterned simultaneously using the CDC method.**

The top layer was a 10  $\mu\text{m}$  (wet thickness) solution of 13.5% w/w gelatin, 0.1% w/w blue dye, and 0.01% w/w 10G. The middle layer was a 10  $\mu\text{m}$  thick solution of 13% w/w gelatin, 0.1% w/w yellow dye and 0.001% w/w 10G. The bottom layer was an 80  $\mu\text{m}$  thick solution of 4.5% w/w gelatin and 0.1% w/w red dye. (a) Full pattern. (b) Close-up of two cells. [Color figure can be viewed in the online issue, which is available at [www.interscience.wiley.com](http://www.interscience.wiley.com).]

hopper coating where the accessible range of wet thickness varies from around 5 to of order 150  $\mu\text{m}$ . Screen-printing is the only other method that can pattern comparable thickness, but may require multiple passes. Multiple passes require accurate registration, and errors associated with this process lead to a decrease in the resolution attainable. With CDC, additional layers are automatically in registry with the original dried layer, which allows for further increase in the thickness of the patterned layers.

We have also shown that CDC can be used to pattern multiple layers simultaneously with the same pattern. This multi-layer capability is unique to CDC. Other patterning technologies require each layer to be applied separately and with registration. The ability to pattern thick liquid layers is potentially useful for a wide range of applications, such as the creation of micro-lens arrays<sup>27</sup> and large-scale flexible display manufacture, where low to medium resolution features are required. The technique may also be used in combination with more standard methods such as screen-printing and vapor deposition to create complex functional structures.

## Acknowledgments

The authors thank Kodak European Research for permission to publish this work.

## Literature Cited

- Weigl BH, Bardell RL, Cabrera CR. Lab-on-a-chip for drug development. *Adv Drug Deliv Rev*. 2003;55:349–377.
- Wang ZJ, Zheng ZH, Li HW, Huck WTS, Sirringhaus H. Dewetting of conducting polymer inkjet droplets on patterned surfaces. *Nat Mater*. 2004;3:171–176.
- Sirringhaus H, Kawase T, Friend RH, Shimoda T, Inbasekaran M, Wu W, Woo EP. High-resolution inkjet printing of all-polymer transistor circuits. *Science*. 2000;290:2123–2126.
- Blake TD, Bonnist E, Bower CL, Simister EA. Method of Pattern Coating. World Patent WO2005014184 [2006].
- Defay R, Prigogine I, Bellemans A, Everett DH. *Surface Tension and Adsorption*. London: Longmans, 1966:61.
- Zisman WA. Relation of the liquid contact angle to liquid and solid constitution. In: Gould RF, editor. *Contact Angle, Wettability, and Adhesion (Advances in Chemistry Series 43)*. Washington, DC: American Chemical Society, 1964:1–51.
- Zisman WA, Shafrin EG. Upper limits to contact angles of liquids on solids. In: Gould RF, editor. *Contact Angle, Wettability, and Adhesion (Advances in Chemistry Series 43)*. Washington, DC: American Chemical Society, 1964:145–157.
- Berg JC, editor. *Wettability (Surfactant Science Series, Vol. 49)*. New York: Marcel Dekker, 1993: Ch. 1 and 5.
- Kwok DY, Li A, Lam CNC, Wu R, Zschoche S, Pöschel K, Gietzelt, T Grundke K, Jacobasch H-G, Neumann WA. Low-rate dynamic contact angles on poly[styrene-alt-(hexyl/10-carboxydecyl (90/10)maleimide)] and the determination of solid surface tensions. *Macromol Chem Phys*. 1999;200:1121–1133.
- Lipowsky R. Morphological wetting transitions at chemically structured surfaces. *Curr Opin Colloid Interface Sci*. 2001;6:40–48.
- Xia Y, Whitesides GM. Soft lithography. *Annu Rev Mater Sci*. 1998; 28:153–184.
- Tadanaga K, Morinaga J, Minami T. Formation of superhydrophobic-superhydrophilic pattern on flowerlike alumina thin film by the sol-gel method. *J Sol-Gel Sci Technol*. 2000;19:211–214.

13. Hens J, Van Abbenyen W. Slide coating. In: Kistler SF, Schweizer PM, editors. *Liquid Film Coating*. London: Chapman and Hall, 1997:427–462.
14. Redon C, Bouchard-Wyart F, Rondelez F. Dynamics of dewetting. *Phys Rev Lett*. 1991;66:715–718.
15. Blake TD, De Coninck J. The Influence of solid/liquid interactions on dynamic wetting. *Adv Colloid Interface Sci*. 2002;96:21–36.
16. Oner D, McCarthy TJ. Ultrahydrophobic surfaces. Effects of topography length scales on wettability. *Langmuir*. 2000;16:7777–7782.
17. <http://www.rkprint.com>.
18. Podgorski T, Flesselles JM, Limat L. Corners, cusps, and pearls in running drops. *Phys Rev Lett*. 2001;87:036102–036105.
19. Blake TD, Ruschak KJ. A maximum speed of wetting. *Nature*. 1979;282:489–491.
20. Hedeström G. On the influence of thin surface films on the evaporation of water. *J Phys Chem*. 1924;28:1244.
21. Greener J, Contestable BA, Balef MD. Interaction of anionic surfactants with gelatin: viscosity effects. *Macromolecules*. 1987;20:2490–2498.
22. Balinov B, Olsson U, Merman O. Structural similarities between the L3 and bicontinuous cubic phases in the AOT-brine system. *J Phys Chem*. 1991;95:5931–5936.
23. Salima Rafai, Dipak Sarker, Vance Bergeron, Jacques Meunier, Daniel Bonn. Superspreading: aqueous surfactant drops spreading on hydrophobic surfaces. *Langmuir*. 2002;18:10486–10488.
24. Brochard-Wyart F, Redon C. Dynamics of liquid rim instabilities. *Langmuir*. 1992;8:2324–2329.
25. Tricot Y-M. Surfactants: static and dynamic surface tension. In: Kistler SF, Schweizer PM, editors. *Liquid Film Coating*. London: Chapman and Hall, 1997:99–136.
26. Padday JF, Pitt AR. Surface and interfacial tensions from the profile of a sessile drop. *Proc R Soc London A*. 1972;329:421–431.
27. Sadik E, Hartmann D, Kibar O. Precision fabrication of diverse polymer microstructures by use of the hydrophobic effect. World Patent WO2001062400 [2001].

Manuscript received Nov. 6, 2006, and revision received Mar. 16, 2007.